JCSE The Journal of Corrosion Science and Engineering
ISSN 1466-8858 Volume 13, Preprint 30 submitted 7 July 2010

Fabrication of three type of Phosphoric Iron and Evaluation of there Mechanical and Corrosion Behavior

Anup Kumar Verma[a]*, Gadadhar Sahoo[b] and Satya Prakash[a],

[a]Metallurgical and Materials Enggineering Department, Indian Institute of Technology, Roorkee, , India

[b]CA&CE Group, R&D Center for Iron and Steel, SAIL, Ranchi-834002, India

*Corresponding author: Anup Kumar Verma, Tele. +91-9305965796

E-mail address: anupverma85@gmail.com

Abstract

The possible use of phosphoric irons for corrosion resistant applications has been addressed. Three phosphoric irons (Fe-0.29P-0.034C, Fe-0.30P-0.030C and Fe-0.31P-0.23C, wt %) were ingot melted and casted. The phosphoric iron were soaked for two hours and then forged between 1050^0C and 1150^0C in the dual phase region to avoid grain boundary embrittlement. The mechanical properties of the low carbon and high carbon phosphoric irons were comparable. The corrosion properties were determined in 3.5 % NaCl solution of pH 6.8. The improved corrosion resistance of phosphoric irons has been understood based on presence of phosphorus in solid solution. The fracture surfaces of three types of phosphoric iron were examined in SEM using back scattered electrons.

Key words: Phosphoric iron, mechanical properties, Polarization, Corrosion.

1. Introduction

The Delhi Iron Pillar has been a center of attraction for engineers, especially corrosion technologists, as it has withstood corrosion for the last 1600 years. The presence of relatively high phosphorus content (0.25 wt. %) in the Pillar leads to the formation of a protective surface film that results in its excellent corrosion resistance [1, 2]. This provides the impetus for developing phosphorus-containing iron or phosphoric irons for modern engineering applications. However, phosphorus is traditionally known to be detrimental to the mechanical properties of

ISSN 1466-8858 Volume 13, Preprint 30 submitted 7 July 2010

steel and is therefore avoided in modern steel making. The brittleness of phosphorus-containing steel arises due to grain boundary segregation of phosphorus. This normally occurs during prolonged exposure and tempering of phosphorus-containing steel in the temperature range 250–600^{0}C and the phenomenon is known as temper embrittlement. Phosphorus also increases the ductile-to brittle transition temperature of steel [3, 4]. The presence of a small amount of carbon displaces phosphorus from grain boundaries by a site competition effect [5, 6]. Therefore, by proper selection of the carbon content in phosphoric irons, ductility can be obtained. In addition, by suitable soaking at high temperature of the (α + γ) dual phase region in the Fe–P phase diagram, phosphorus can be kept away from grain boundaries and significant toughness can be obtained [7].

Corrosion of reinforcement bars in concrete structures is a major worldwide problem, especially in marine environments and locations where deicing salts are used. A significant amount of economic loss occurs due to premature failure of structures because of degradation by corrosion. For example, in the US, during the period 1992–1999, between 15% and 20% of all bridges were listed as ‘‘structurally deficient” (i.e. they can no longer sustain the loads) due to damage caused by chloride-induced corrosion of rebars [8]. The estimated annual direct cost of bridge infrastructure corrosion to the US economy was estimated at $8.3 billion per annum and the indirect cost was reported to be many times higher [8]. There is, therefore, always a need to develop corrosion resistant bars for concrete reinforcement applications. Given the excellent atmospheric corrosion resistance of phosphoric irons in environments laden with chlorides, as revealed by the good corrosion resistance of ancient phosphoric iron beams at Konark and Puri (both cities are located on the eastern seacoast of the Indian subcontinent) [9], it suggested that phosphoric irons can be considered as candidate materials for concrete reinforcement applications, specifically in environments where chloride content is high. The phosphoric irons may not be susceptible to stress corrosion cracking like prestressed steels and high strength steels, because the strength and ductility of phosphoric irons is similar to that of mild steel used for concrete reinforcement application [10]. Therefore, the stress corrosion cracking phenomena in phosphoric irons can be anticipated to be similar to that of mild steel in the concrete environment. The necessary strength can be obtained in phosphoric irons because phosphorus is a good solid solution strengthening element in iron [11, 12]. The presence of P also promotes marked work hardening. However, Phosphorus promotes cold shortness or brittleness during

ISSN 1466-8858 Volume 13, Preprint 30 submitted 7 July 2010

cold working due to segregation to grain boundaries [13-15]. Due to this deleterious effect, concentration of phosphorus is maintained less than 0.05 % in modern steel making [16]. The deleterious effect of P on ductility can be minimized by maintaining a low amount of carbon, preferably at the grain boundaries and by appropriate heat treatments [7, 12, 17].

The aim of the present study is to explore the mechanical behavior of phosphoric iron and its corrosion behavior in 3.5 % NaCl solution of pH 6.8 (marine environment).

2. Experimental

Three square plates (5 cm height and 50 cm^2 cross section) of Fe-C-P alloys of different compositions were prepared in a 500 kg capacity induction melting furnace (at Vaishnav steel Pvt Ltd, Mujaffarnagar) in air by the addition of a ferro-phosphorus alloy to the soft iron, Some aluminum shots were added during pouring of melt into mould for reducing the oxygen content in the melt, which possessed similar impurities like in mild steel. Some steel scraps were also added to balance the carbon concentration. The square plates were named as sample P_1 (Fe-0.29P-0.034C), sample P_2 (Fe-0.30P-0.030C) and sample P_3 (Fe-0.31P-0.23C). All the compositions mentioned in this paper are in wt%. The compositions were determined using spectroscopy and are provided in Table 1. As carbon is an interstitial solute and Phosphorous is a substitutional solid solute, they will avoid each other. In case carbon can be segregated to the grain boundaries, it will further result in minimizing P segregation to the grain boundaries.

The square plates were cut into smaller sizes and these pieces were provided a homogenization treatment by soaking at 1150^0C for two hours. They were then forged into 25 mm thickness plates in the temperature range 1050^0C to 1150^0C at the Metal Forming Laboratory, IIT Roorkee. Based on the Fe-P phase diagram, which reveals a gamma loop at high temperature (Fig. 1), the temperature range of 1050^0C-1150^0C corresponds to the dual phase (ferrite and austenite) region. The purpose behind heat treating phosphoric iron in the dual phase region has been explained in detail elsewhere [18]. The purpose of soaking ingots at 1150 ^{0}C was, first, to remove macro-segregation of phosphorus, and secondly, to attain a duplex microstructure. The high-temperature γ-loop region of the Fe–P phase diagram (Fig. 1) provides that phosphoric iron will remain in the (α + γ) dual phase region during soaking at 1150 ^{0}C.

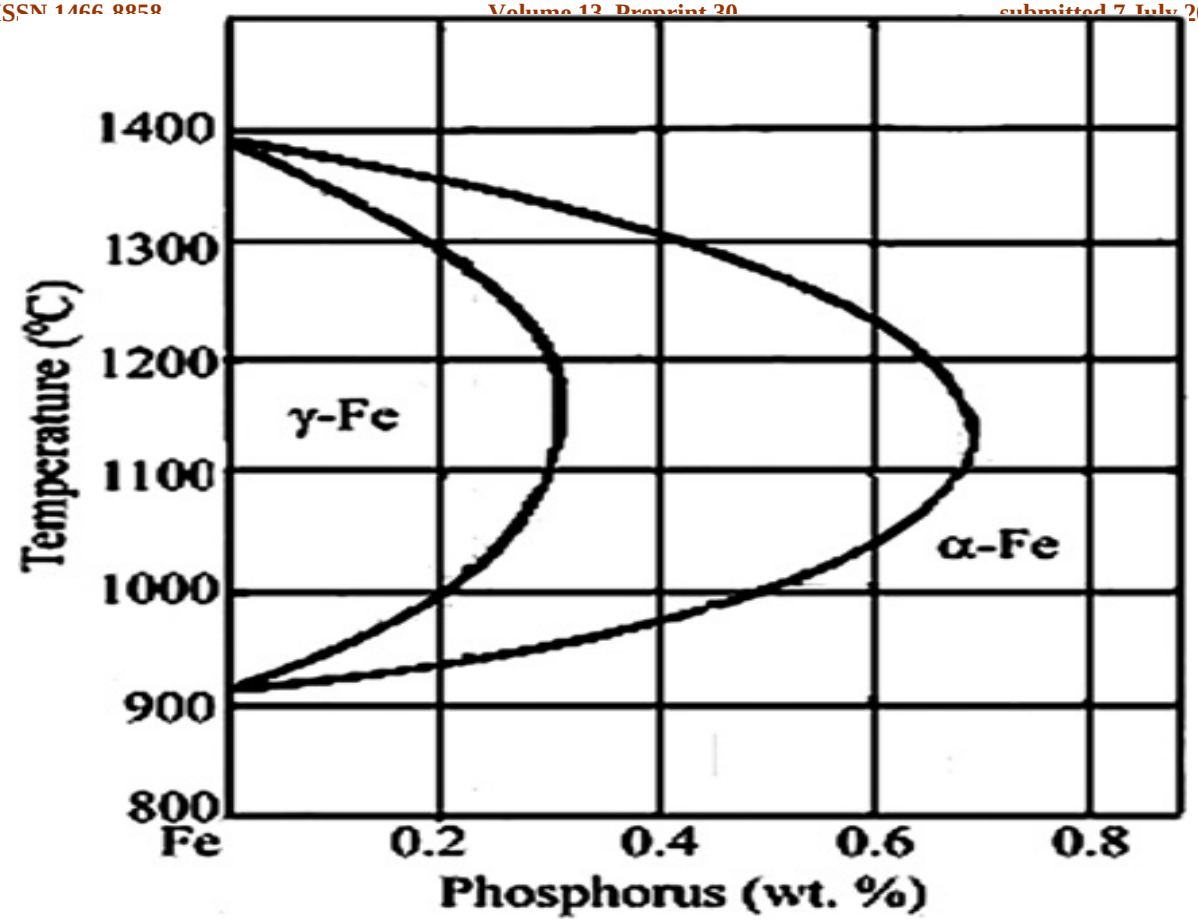

Fig .1 High temperature gamma loop region of Fe-P phase diagram, after Kubaschewski [19].

The basic philosophy was to precipitate austenite along the grain boundaries which results in lower phosphorous content at these regions due to the lower solubility of phosphorus in austenite. On cooling down, this inhomogeneous phosphorus distribution remains. This is anticipated to improve ductility because phosphorus would be avoided at grain boundary locations. The microstructures of the forged samples were understood using Oberhoffer and 3% nital as etchants. The usefulness of using the Oberhoffer etchant (500 ml H_2O + 30 g $FeCl_3$ + 0.5 g $SnCl_2$ + 1 g $CuCl_2$ + 500 ml C_2H_5OH + 50 ml HNO_3) to reveal phosphorus compositional inhomogenities has been explained elsewhere [20].

ISSN 1466-8858 Volume 13, Preprint 30 submitted 7 July 2010

Table 1. Average composition of phosphoric iron.

Samples	C	P	Si	Mn	S	Ni	Cr	Mo	V	Cu
P_1	0.034	0.29	0.14	0.166	0.009	0.022	0.039	0.005	0.006	0.029
P_2	0.030	0.30	0.03	0.133	0.008	0.026	0.118	0.006	0.006	0.029
P_3	0.226	0.30	0.159	0.223	0.009	0.026	0.145	0.005	0.001	0.031

The mechanical properties of the samples were also evaluated. Hardness of each sample was obtained at least 5 times in a Vickers hardness testing machine. Tensile tests were performed using cylindrical test specimens as per ASTM-A370 standard (diameter 4 mm and gauge length 16 mm). The tensile test pieces were strained at room temperature (27^0C) in a Hounsfield tensile machine (model H 20 K-W) of 20 kN capacity using a strain rate of 1.6×10^{-3} s^{-1}. This strain rate lies in the regime for 'static' tension test. The fracture surfaces were examined in an FEI QUANTA 200 SEM using back scattered electrons.

The electrochemical behavior of the samples was studied in a standard flat cell (EG & G, USA) in freely-aerated 3.5% NaCl solution of pH 6.8, using silver-silver chloride electrode (SCC) as reference. The samples were polished up to 800 grade silicon carbide paper and degreased with acetone and finally washed with distilled water before each experiment. Tafel polarization studies were performed in 3.5% NaCl using a scan rate 0.166 mVs^{-1} solution using a computer controlled potentiostat (PARSTAT 2263, EG & G, USA). All the experiments were repeated three to four times.

3. Results and Discussion

3.1. Microstructural Characterization

The as-received specimens (P_1, P_2 and P_3) were hot forged after soaking the plates in dual phase ($\alpha+\gamma$) region. It resulted in austenite forming along the grain boundaries of ferrite after etching with Nital.

The microstructure of specimen (P_1, P_2 and P_3) of phosphoric iron were normalized (i.e. air cooled), after soaking at 1150^0C for 2 hrs respectively are shown in Fig. 2(a), 2(b) and 2(c) respectively. This duplex microstructure consisted of prior austenite at the grain boundaries of ferrite.

JCSE The Journal of Corrosion Science and Engineering
ISSN 1466-8858 Volume 13, Preprint 30 submitted 7 July 2010

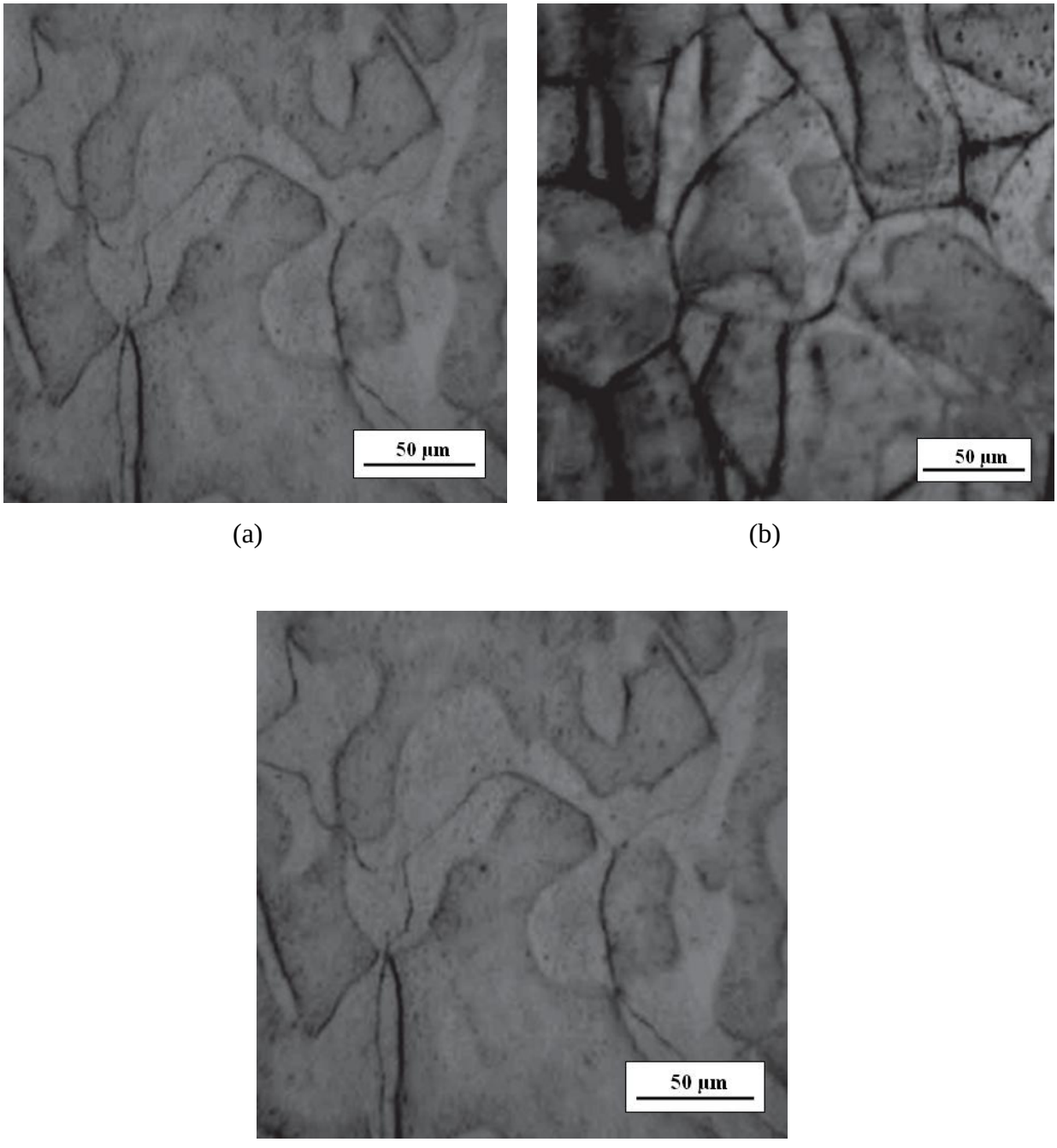

(a) (b)

(c)

Fig. 2 Optical micrograph showing prior austenite in the grain boundary ferrite for samples P_1 (a), P2 (b), P_3 (c).

JCSE The Journal of Corrosion Science and Engineering
ISSN 1466-8858 Volume 13, Preprint 30 submitted 7 July 2010

3.2. Mechanical Behavior

3.2.1. Hardness

Hardness was evaluated with the help of a Vickers Hardness Tester using a load of 10 kg. The five indentations were taken to estimate the average value of hardness of the phosphoric iron under investigation. The measured hardness (Vicker's hardness number, VHN) for the specimens of P_1, P_2 and P_3 are provided in Table 2.

Table 2. Average hardness of specimens after soaking two hour at temperature 1150^0C.

Specimens	Hardness (VHN)
P_1	164.4
P_2	162.2
P_3	151.4

The variation of hardness of the different samples is shown in Fig. 3. The hardness of samples P_1 and P_2 are comparable because both are approximately equal composition. The hardness of P_3 sample is less. As the carbon content increases, the hardness of the sample decreases is shown in the Fig. 3.

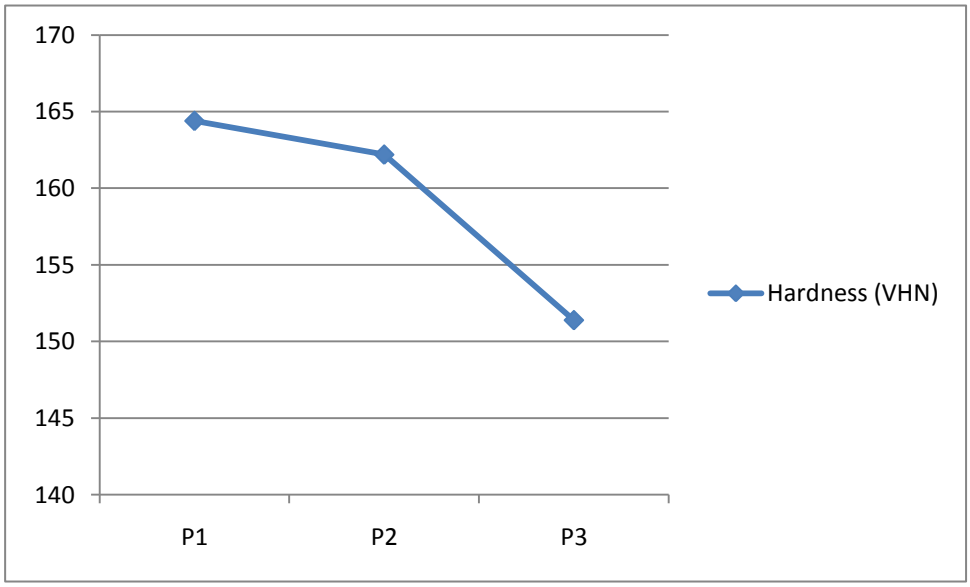

Fig. 3 Comparison of different composition as a function of Hardness (VHN).

JCSE The Journal of Corrosion Science and Engineering
ISSN 1466-8858 Volume 13, Preprint 30 submitted 7 July 2010

3.2.2 Tensile Test

The stress strain curve of specimen P_1, P_2 and P_3 are shown in Fig. 4(a), 4(b), and 4(c), respectively. Table 3 is showing the tensile properties of the specimens. The proof stress and ultimate tensile stress of specimen $P_1$and P_2 are almost similar and is high for specimen P_3. As the carbon content of the phosphoric iron increases, the proof stress and ultimate tensile stress of specimen increases. The ultimate tensile stress of phosphoric increased with increasing carbon content (Table. 3), similar to that reported by Hopkins and Tipler [16] and steewart et al. [7].

Typical fractographs of specimen P_1, P_2 and P_3 are shown in Fig. 5(a), 5(b), and 5(c), respectively. The fracture surface of the samples revealed conical equiaxed dimples, which is generally expected for ductile specimens that fail under uniaxial tension [21]. But, the failure mode of the samples was mixed, i.e. brittle-cleavage rupture with some dimple rupture.

Table 3. Tensile properties of samples (Samples air-cooled after soaking for 2 hour at 1150^0C).

Expt. No.	Proof Stress (MPa)	Ultimate Tensile Stress (MPa)	% Elongation at failure
P_1	351.1	432.4	12.60
P_2	318.5	505	19.47
P_3	422.8	637	18.91

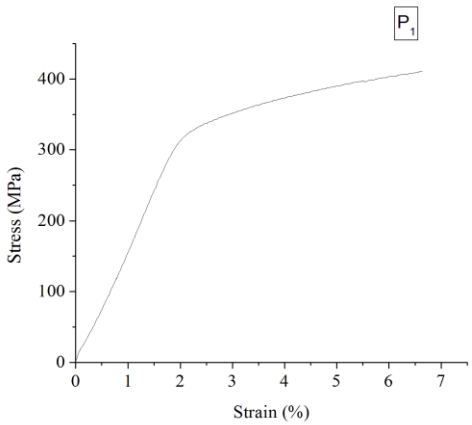

(a)

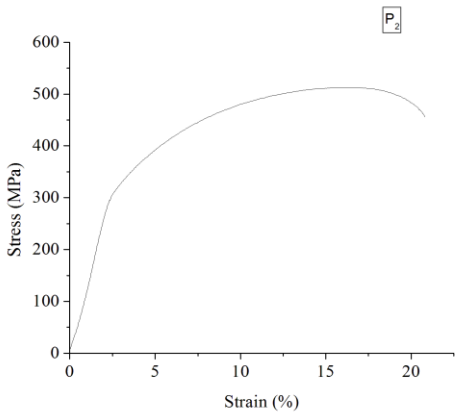

(b)

JCSE The Journal of Corrosion Science and Engineering
ISSN 1466-8858 Volume 13, Preprint 30 submitted 7 July 2010

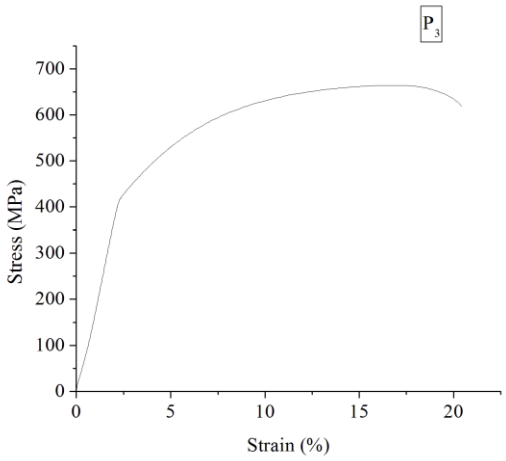

(c)

Fig. 4 Stress Strain curves of the sample P_1 (a), P_2 (b), P_3 (c).

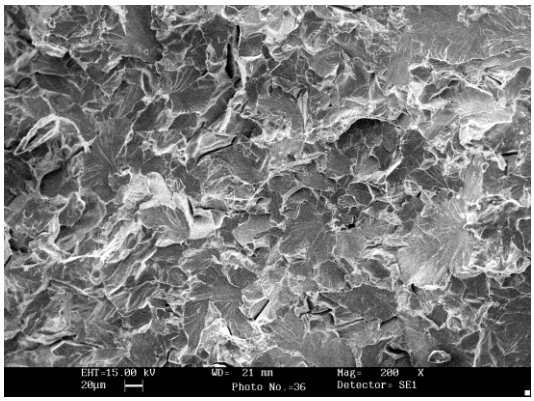

(a)

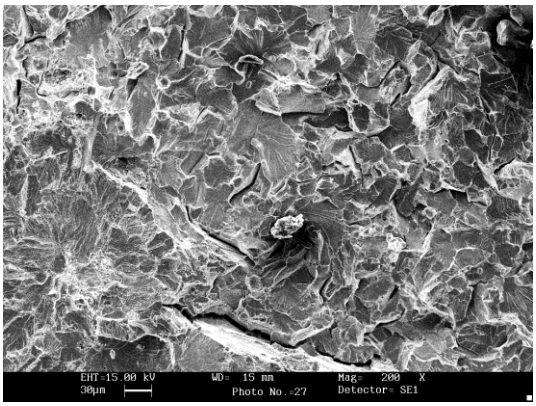

(b)

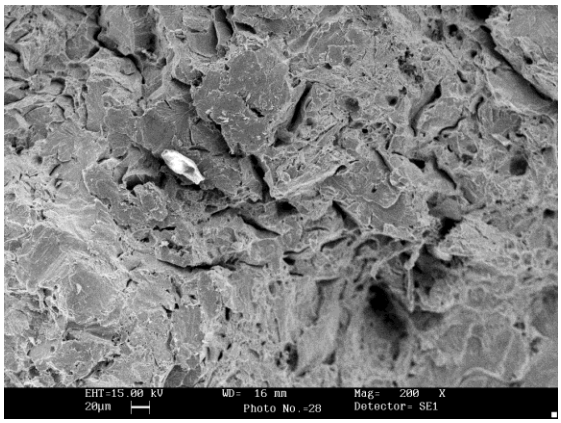

(c)

Fig. 5 SEM micrographs of the fracture surface of tensile sample P_1 (a), P_2 (b), P_3 (c).

JCSE The Journal of Corrosion Science and Engineering
ISSN 1466-8858 Volume 13, Preprint 30 submitted 7 July 2010

3.3 Electrochemical Behavior

The corrosion rate obtained from Tafel plot of the rusted samples are provided in Table 4. The samples P_1 and P_2 exhibit almost similar corrosion rates and P_3 exhibit the high corrosion rate. The corrosion rate increased with increasing carbon content. The corrosion rate are comparable with corrosion rate of pure iron obtained by Tafel extrapolation in unstirred, air saturated 3.5 % NaCl solution, which is 12 mpy.

Table 4. Tafel parameters, i_{corr} and corrosion rate (mpy) obtained from Tafel plot in aerated, unstirred 3.5 % NaCl solution.

Sample	Ba (mV/dec)	Bc (mV/dec)	ZCP_{SCE} (mV)	i_{corr} ($\mu A/cm^2$)	Corrosion Rate (mpy)
P_1	14.73	755.49	-499.21	3.64	6.09
P_2	17.937	585.312	-570.322	3.26	5.60
P_3	7.346	1185.46	-471.21	4.89	8.19

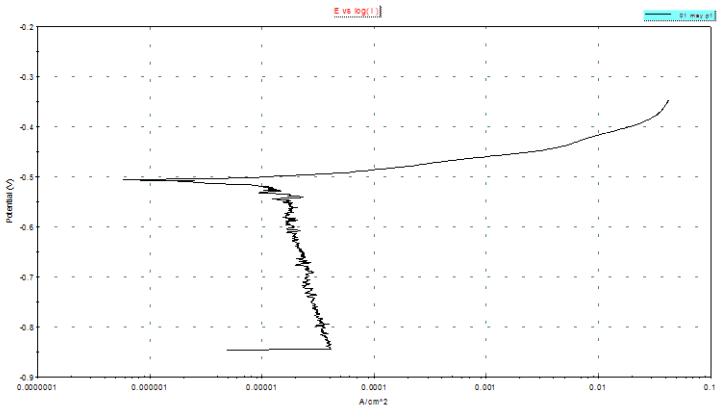

Fig.6 (a) Tafel extrapolation curve for sample P_1 in 3.5 % NaCl solution.

JCSE The Journal of Corrosion Science and Engineering
ISSN 1466-8858 Volume 13, Preprint 30 submitted 7 July 2010

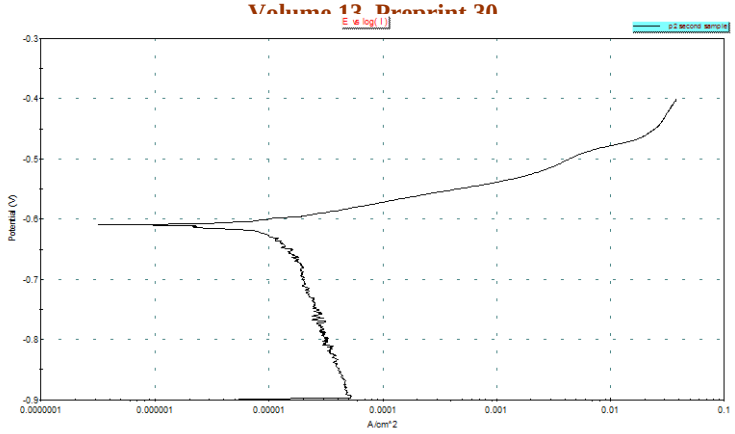

Fig.6 (b) Tafel extrapolation curves for sample P_2 in 3.5 % NaCl solution.

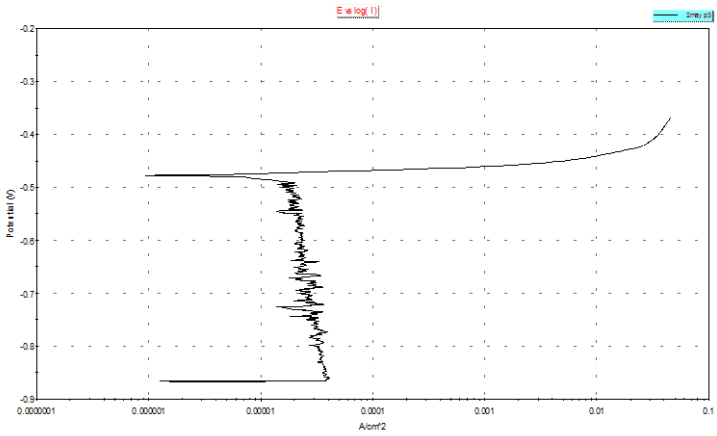

Fig.6 (c) Tafel extrapolation curves for sample P_3 in 3.5 % NaCl solution.

4 Conclusions

The possible use of phosphoric iron for corrosion resistance application has been studied. Three phosphoric iron of composition Fe-0.29P-0.034C, Fe-0.30P-0.030C and Fe-0.31P-0.23C were melted and casted and then evaluated with respect to mechanical and electrochemical behavior in 3.5% NaCl solution of pH 6.8. The salient conclusions of the study are:

1. As received phosphoric iron P_1, P_2 and P_3 soaked and forged in the (α+γ)-dual phase region after etching with Nital in Fe-P phase diagram revealed duplex microstructure. This duplex microstructure consisted of prior austenite at the grain boundaries of ferrite.

ISSN 1466-8858 Volume 13, Preprint 30 submitted 7 July 2010

2. Inhomogeneity of phosphorus distribution was observed with Nital etchant. The segregation of P to grain boundary region was avoided by forging in the two phase region.
3. As the carbon content of the phosphoric iron increases, the proof stress and ultimate tensile stress of specimen increases.
4. The failure mode was mixed, i.e. brittle-cleavage rupture with some dimple rupture.
5. The samples P_1 and P_2 exhibit almost similar corrosion rates and P_3 exhibit the high corrosion rate. The corrosion rate increased with increasing carbon content. The corrosion rate are comparable with corrosion rate of pure iron obtained by Tafel extrapolation in unstirred, air saturated 3.5 % NaCl solution, which is 12 mpy.

Acknowledgement

The author acknowledges Vaishnav Steel Pvt Ltd, Muzzafarnagar (U.P.) for melting and casting of the phosphoric iron samples.

References

[1] ‘On the corrosion resistance of the Delhi iron pillar’, R. Balasubramaniam, Corrosion Science, **42,** pg 2103, 2000.

[2] ‘Characterization of Delhi iron pillar rust by X-ray diffraction, Fourier transform infrared spectroscopy and Mossbauer spectroscopy’, R. Balasubramaniam, A.V. Ramesh Kumar, Corrosion Science, **42,** pg 2085, 2000.

[3] ‘The fracture behavior of quenched and tempered manganese steel’, Metallurgical Transactions A: Physical Metallurgy and Materials Science, C.L. Briant, S.K. Banerji, **13**, pg 827, 1982.

[4] ‘Tempered martensite embrittlement in SAE 4340 steel’, J.P. Materkowski, G. Krauss, Metallurgical Transactions A: Physical Metallurgy and Materials Science, **10A**, pg 1643, 1979.

[5] ‘Role of carbon in preventing the intergranular fracture in Fe-P alloy’, S. Suzuki, K. Abiko, H. Kimura, Transactions ISIJ, **25**, pg 62, 1985.

[6] 'Equilibrium segregation of phosphorus at grain boundaries of iron-phosphorus, iron-carbon-phosphorus, iron-chromium-phosphorus, and iron-chromium-carbon-phosphorus alloys', H. Erhart, H.J. Grabke, Metal Science, **15**, pg 401, 1981.

[7] 'Iron–phosphorus system Part 1- Mechanical properties of low carbon Fe-P alloys', J.W. Stewart, J.A. Charles, E.R. Wallach, Material Science and Technology, **16**, pg 275, 2000.

[8] 'Prevention of chloride-induced corrosion damage to bridges, S.D. Cramer, B.S. Covino, S.J. Bullanrd, G.R. Holcomb, J.H. Russell, M. Zimolek-moroz, Y.P. Voramo, J.T. Bulter, F.J. Nelson, N.G. Thompson, ISIJ Int. **42**, pp 1376–1385, 2002.

[9] 'Delhi Iron Pillar: New Insight', R. Balasubramaniam, Indian Institute of Advanced Studies and Aryan Books International, New Delhi, Shimla, pp 138–139, 2002.

[10] 'Mechanical behavior of novel phosphoric irons for concrete reinforcement applications', Gadadhar Sahoo and R. Balasubramaniam, Scripta Materialia, **56**, pp 117–120, 2007.

[11] 'Effect of phosphorus on microstructure and strength of high carbon steel rod', B. Clarke and I. Mcivor, Iron making Steel, **16**, pp 335-344, 1989.

[12] 'In Iron and its dilute solid solutions', N. Allen, Willey Interscience, New York, pp 271-308, 1963.

[13] 'Interaction of phosphorus, carbon, manganese, and chromium in intergranular embrittlement of iron', Y. Wang, C. Mcmahon, *Material Science Tenchnology*, **3**, pp 207-216, 1987.

[14] 'Phosphorus in low carbon iron: Its beneficial properties' M. Goodway, R. M. Fisher, Historical Metallurgy, **22**, pp 21-23, 1988.

[15] G. E. Dieter, Mechanical Metallurgy, SI Metric Edition, McGraw Hill Nework, pp 295-297 and 478-485, 1988.

[16] 'The effect of phosphorus on the tensile and notch-impact properties of high-purity iron and iron–carbon alloys', B.E. Hopkins, H.R. Tipler, J. Iron Steel Inst. **188**, pp 218–237, 1958.

[17] 'Role of carbon in preventing the intergranular fracture in Fe-P alloys', S. Suzuki, M. Obata, K. Abiko and H. Kimura, Transactions ISIJ, **25**, pp 62-68, 1985.

[18] 'Characterzation of rust on ancient Indian iron', R. Balasubramaniam, Current Science, **85**, pg 9, 2003.

[19] 'Iron-Binary Phase Diagrams', O. Kubaschewski, Springer Verlag, Berlin, pg 84, 1982.

ISSN 1466-8858 Volume 13, Preprint 30 submitted 7 July 2010

[20] 'Iron–phosphorus system Part-3 metallography of low carbon Fe-P alloy', J.W. Stewart, J.A. Charles, and E. R. Wallach, Material Science and Technology, **16**, pp 275-282, 2000.

[21] 'Fractography, in: ASM Hand Book The Materials Information Society', V. Kerlins, A. Philips, ASM International, Materials Park, OH, **12**, pg 12, 1999.